Rothamsted Repository Download

A - Papers appearing in refereed journals

The publisher's version can be accessed at:

- https://doi.org/10.1111/1365-2664.70009

The output can be accessed at: https://repository.rothamsted.ac.uk/item/99226/early-detection-strategies-for-invading-tree-pests-targeted-surveillance-and-stakeholder-perspectives.

SUPPLEMENTARY INFORMATION

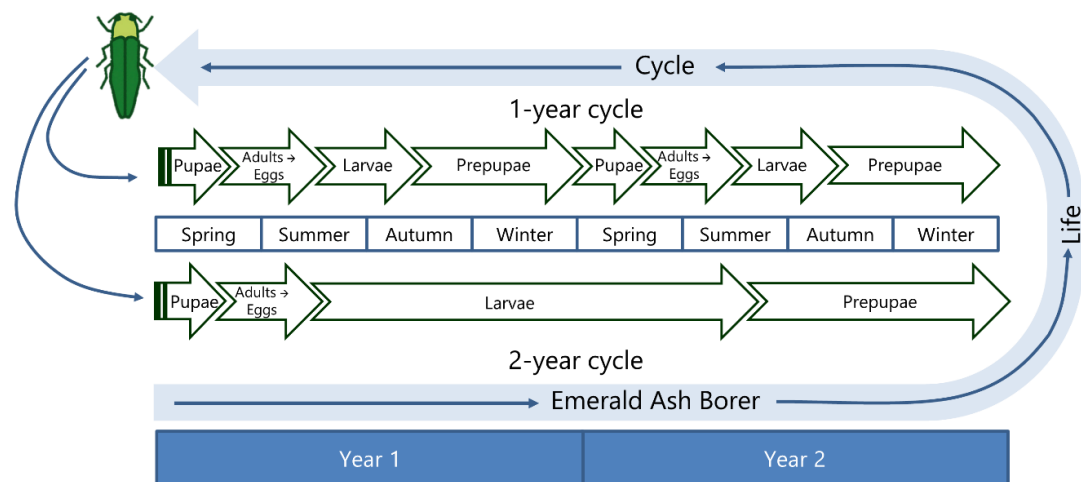## S1: SUPPLEMENTARY FIGURES

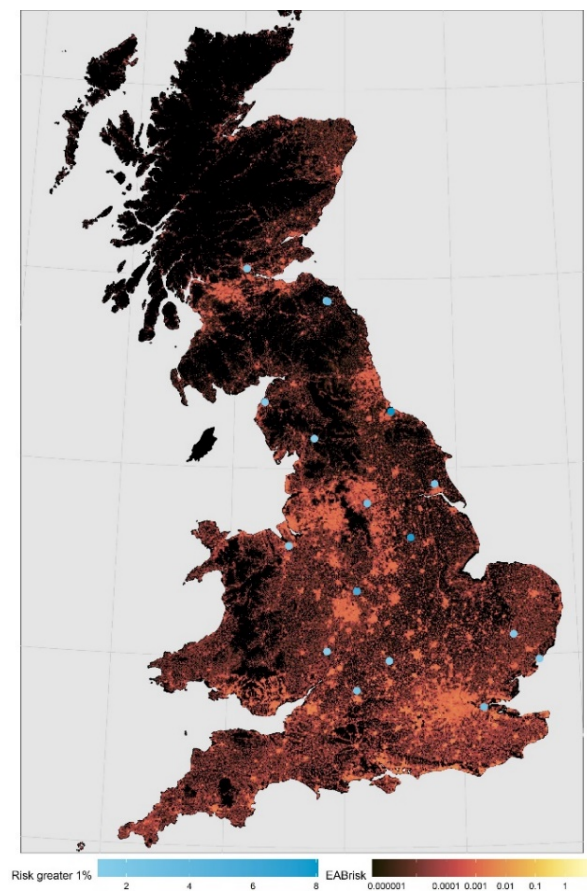Figure S1.1: The lifecycle of EAB.

Figure S1.2: Predictions of entry point probability where the confidence in the knowledge of EAB arrival pathway is 70%. Blue dots indicate areas where the probability is greater than 0.01 under this scenario.

S2: POPULATION DYNAMICS OF EAB MODEL

We consider that EAB has either a one- or two-year lifecycle as shown in Figure 2 of the main text. To track a single population over time we assume that there is a fraction $1 - \theta$ of the larvae that mature in a one-year cycle, and the rest θ matures the following year. This couples the years and the populations.

Following (Duan et al., 2013) we assume that the EAB larvae population survival is density dependent. The main effect contributing to this density dependence is cannibalism, in addition to a non-density-dependent death rate. This non-density-dependent death rate can be attributed, for example, to larvae starvation, tree defence mechanisms, etc.

Once EAB infests the ash tree population we can categorise trees into infested and un-infested. Then we estimate the total number of adults in a 1 km^2 cell by adding up all the EAB adults emerging from all the infested trees in that cell. Infested trees are then separated into two groups, those infected for the first time in the ongoing year, and those infested for more than one year. This is because for trees in the first year of infestation, only adults from larvae in their first-year life cycle emerge while in the rest of the trees, larvae are going through one- and two-year life cycles.

S2.1 Larvae survival through the year

$L_t(\tau)$ represents the total number of larvae in life cycle t at time τ, with τ going from $\tau = 0$ (oviposition) to $\tau = T$ (adult emergence). As the density-dependent larval density decreases with cannibalism, α, and with an additional density-independent death rate, ω, we can write

$$\frac{d\, L_t(\tau)}{dt} = -\alpha L^2 - \omega L \#(S2.1.1)$$

Assuming that $L_t(0) = L_0$, is the initial number of larvae produced by the adults in year t we can solve (S2.1.1) to obtain

$$L_t(T) = \frac{e^{-\omega T} L_t(0)}{1 + \frac{\alpha}{\omega}(1 - e^{-\omega T}) L_t(0)} \#(S2.1.2)$$

Rewriting $\beta = e^{-\omega T}$ and $\gamma = \frac{\alpha}{\omega}(1 - e^{-\omega T})$, we obtain $\quad L_t(T) = \frac{\beta\, L_t(0)}{1 + \gamma L_t(0)} \#(S2.1.3)$

So, the probability that a larva survives until the end of its lifecycle, f, is

$$f(\overline{L}) = \frac{\beta \overline{L}}{1 + \gamma \overline{L}} \#(S2.1.4)$$

where $\overline{L}$ is the total larvae population, the sum of the first- and second-year larvae, i.e., $\overline{L} = U_t + L_t$. The reason for this rewrite becomes clear in the next section.

S2.2 Adults and reproduction

The number of adults per meter square of phloem at the start of year n is $A_n/(\phi \cdot I_n)$ where A_n is the total of adults among trees, I_n the number of infested trees and ϕ the phloem area of an average tree. The probability for an adult individual to die before it reproduces is σ, so it has a probability $(1 - \sigma)$ to reproduce. Each adult produces ϑ eggs from which k survive to the larvae stage. Thus, $U_t(0) = (1 - \sigma)k\frac{A_t}{\phi \cdot I_t}$ where U_t refers to larvae per tree in their first cycle and $\kappa = (1 - \sigma)k$. We denote larvae in their second year by L_t .

S2.3 Larvae and adult populations

As $\bar{L} = U_t + L_t$ and assuming that all larvae cannibalise at the same rate, α, and are under the same additional death rate, ω, then the number of adults a_{t+1} emerging from a single infested tree that has been infested for more than one year is given by

$$a_{t+1}^{(2)} = ((1 - \theta)U_t + L_t)\frac{f(\bar{L})}{\bar{L}} = \frac{((1 - \theta)U_t + L_t)\beta(U_t + L_t)}{(U_t + L_t)(1 + \gamma(U_t + L_t))} \#(S2.3.1)$$

where

$$L_{t+1} = \theta\frac{U_t}{\bar{L}}f(\bar{L}) = \theta\frac{U_t\beta(U_t + L_t)}{(U_t + L_t)(1 + \gamma(U_t + L_t))}\#(S2.3.2)$$

While the number of adults emerging from a single tree infested for only one year is

$$a_{t+1}^{(1)} = (1 - \theta)\frac{U_t}{U_t}f(U_t) = (1 - \theta)f(U_t) = (1 - \theta)\frac{\beta U_t(0)}{1 + \gamma \, U_t(0)}\#(S2.3.3)$$

Substituting $U_t(0)$, we get

$$a_{t+1}^{(2)} = \frac{(1 - \theta)\kappa\beta\dfrac{A_t}{\phi \cdot I_t} + \beta L_t}{1 + \gamma\kappa\dfrac{A_t}{\phi \cdot I_t} + \gamma L_t}\#(S2.3.4)$$

$$L_{t+1} = \theta\frac{\kappa\beta\dfrac{A_t}{\phi \cdot I_t}}{1 + \gamma\kappa\dfrac{A_t}{\phi \cdot I_t} + \gamma L_t}\#(S2.3.5)$$

$$a_{t+1}^{(1)} = (1 - \theta)\frac{\beta\kappa\dfrac{A_t}{\phi \cdot I_t}}{1 + \gamma\kappa\dfrac{A_t}{\phi \cdot I_t}}\#(S2.3.6)$$

S2.4 Population of infested trees

The number of un-infested trees per km^2 in year t and cell (i,j) is denoted by $S_t(i,j)$, the number of infested trees by $I_t(i,j)$ and the total number of adult beetles by $A_t(i,j)$.

The average number of adults landing on an un-infested tree is a function of the total number of adults, $f(A_t)$. Each adult has a probability μ to lay an egg in the tree for the first time and make it an infested tree. The probability to become an infested tree, using the Poisson distribution is then $(1 - e^{-\mu f(A_t)})$.

The function f can have a range of forms and for simplicity we use $f(A_t) = A_t$.

The number of susceptible trees remaining in cell (i,j) in year $t + 1$ is given by

$$S_{t+1}(i,j) = S_t(i,j) \, e^{-\psi A_t(i,j)}\#(S2.4.1)$$

$\psi = \mu\rho$ where μ is the probability of infesting a new tree, and ρ is the proportion of adults landing on an uninfested tree. It follows, therefore, that the number of infested trees in year $t + 1$ is given by

$$I_{t+1}(i,j) = I_t(i,j) + S_t(i,j)(1 - e^{-\psi A_t(i,j)}) \#(S2.4.2)$$

The total number of adults emerging from cell (i,j) is given by

$$E_{t+1}(i,j) = \phi[(I_{t+1}(i,j) - I_t(i,j)) a_{t+1}^{(1)}(i,j) + I_n a_{t+1}^{(2)}(i,j)] \#(S2.4.3)$$

S3: Detection probabilities for different devices

In this section we focus on detecting EAB individuals rather than estimating insect density; therefore, we calculate the probability of the insects' presence (or absence). The reason to do this is that we are trying to maximise the probability of detecting at least one beetle at an early stage of the invasion.

The monitoring methods considered are
1. Traps
2. Tree girdling
3. Under-bark assessment of trees

1. *Traps*

Around a trap there is an EAR (effective attraction radius), so the area around the trap is πEAR^2. When an adult flies into that radius it has a probability ε to end up in the trap.

The area under consideration (in our case a 1 km x 1 km grid cell) is O. In this area there are N_T traps, so the fraction of the area covered by the attraction areas of the traps is $N_T \cdot \frac{\pi EAR^2}{O}$.

The beetles fly at a speed v (km per day). The number of times an insect enters the EAR of a trap is proportional to the flight speed. We assume that each insect flies independently of the others. Therefore, the number of insects entering the EAR of a trap per unit of time for the entire adult population A_t in year t is proportional to $\left(N_T \cdot \frac{\pi EAR^2}{O}\right) \cdot vA_t$. Thus, the mean number of traps catches per time unit is

$$\frac{N_T \cdot \pi \cdot EAR^2}{O} \cdot vA_t\varepsilon \#(S3.1)$$

Then, for the entire trapping period τ, the mean number of traps catches is

$$\frac{N_T \cdot \pi \cdot EAR^2}{O} \cdot vA_t\varepsilon\tau \#(S3.2)$$

Using the Poisson distribution, the probability that the presence of the insect is found P is given by

$$P_t = 1 - \exp\left(-\frac{N_T \cdot \pi \cdot EAR^2}{O} \cdot vA_t\varepsilon\tau\right) = 1 - \exp\left(-c_T N_T A_t\right) \#(S3.3)$$

where $c_T = \frac{\pi\,EAR^2}{O}v\varepsilon\tau$.

2. *Tree girdling*

There is an area Δ around a girdled tree where adult beetles are attracted. The probability of finding the girdled tree when the beetle flies into that area is ε. Again, we consider that the study area is a 1x1 km grid cell denoted by O. The number of girdled trees in that area is N_G, so the fraction of the area covered by the attraction areas of the girdled trees is $\frac{N_G\Delta}{O}$.

The beetles fly with a speed v (km per day) and the number of times a beetle enters the attraction area of a girdled tree Δ, is proportional to the flight speed. Assuming that each individual insect flies independently of the others, the number of insects entering the Δ of a girdled tree per unit of time for the entire adult population A_t in year t is proportional to $\left(N_G \cdot \frac{\Delta}{O}\right) \cdot vA_t$. Thus, the mean number of insects landing on a girdled tree per time unit is

$$\frac{N \cdot \Delta}{O} \cdot vA_t\varepsilon \#(S3.4)$$

Then, for the entire trapping period τ, the mean number of beetles landing on girdled trees is

$$\frac{N \cdot \Delta}{O} \cdot v A_t \varepsilon \tau \#(S3.5)$$

The probability that a beetle lies eggs on the girdled tree and that they are subsequently detected by a surveyor is ζ, so the mean number of larvae detections on girdled trees is $\left(\frac{\zeta N_G \Delta}{O}\right) \cdot v A_t \varepsilon \tau$. Using the Poisson distribution, the probability P that the presence of the insect is found is given by

$$P_t = 1 - \exp\left(-\left(\frac{\zeta N_G \Delta}{O}\right) \cdot v A_t \varepsilon \tau\right) = 1 - \exp(-c_G N_G A_t) \#(S3.6)$$

where $c_G = \left(\frac{\zeta \Delta}{O}\right) \cdot v \varepsilon \tau$.

3. _Under-bark assessment_

The probability that a randomly selected tree is infested is given by p. The probability that an observer recognises that the tree is infested (determined by taking a piece of bark and looking for larvae) is ϖ. If N_B trees are surveyed, then the mean number of infested trees detected is $p \varpi N_B$. If the tree density is Z (number of trees/km^2), where $Z = I + S$, the mean number of adults per infested tree is A/I. The probability that adults infesting a tree lay eggs resulting in larvae to be observed under the bark is ϱ, then the probability that a randomly selected tree is infested in year t is given by

$$p = 1 - e^{-\varrho \frac{A_t}{I_t}} \#(S3.7)$$

Using the Poisson distribution, the probability that the presence of the insect is established, P, when N_U trees are sampled is given by

$$P_t = 1 - \exp\left(-\varpi N_U\left(1 - \exp\left(-\varrho \frac{A_t}{I_t}\right)\right)\right) \#(S3.8)$$

As we are looking for early detection, we can safely assume that the adult's density is small so that $1 - \exp\left(-\varrho \frac{A_t}{I_t}\right) \approx -\varrho \frac{A_t}{I_t}$, obtaining

$$P_t = 1 - \exp\left(-\varpi N_U \varrho \frac{A_t}{I_t}\right) = 1 - e^{-c_B N_B A_t} \#(S3.9)$$

where $c_B = \varpi \varrho / I_t$.

For all methods, the mean number of insects detected is linearly related to the insect density, A_t (for adult) or L_t (for larvae) in year t, multiplied by the observation unit density, N_i where, $i = T, G, B$ the number of traps, girdled trees, or under-bark assessment of trees per unit area. Thus, the probability that during one sampling round the insect is detected is $P_{i,t} = 1 - \exp(-c_i N_i A_t)$ or $P_{i,t} = 1 - \exp(-c_i N_i L_t)$. Where c_i is dependent on the monitoring method.

Obtaining c_i _values_

Using the data obtained by (Siegert et al., 2010a) we calculate the c parameter for traps and girdled trees. For under-bark assessment we use the data from (Mercader et al., 2012), (McCullough & Siegert, 2007) and (Siegert et al., 2010a).

We fit $P_i = 1 - e^{-c_i NL}$, to Figure 2 in (Mercader et al., 2013) f where P_i is the probability to detect EAB with method $i = T, G$ where T denotes traps and G girdled trees and N is the number of the units deployed (so either girdled trees or traps), and L is the number of larvae per tree, when using the number of larvae per tree as population measure (if we use the number of adults then we change L for A). In (Mercader et al., 2013), the density of traps and trees is given

as the number of traps per 2.6 km^2, so if N is in number per one km^2 we obtain $c_G = 0.5096$ and $c_T = 0.052$.

For underbark we use the measure of larvae per square meter of phloem from (McCullough & Siegert, 2007; Mercader et al., 2012; Siegert et al., 2010a) to calculate the number of larvae per tree by multiplying

$$\frac{\text{larvae}}{\text{tree}} = \left(\frac{\text{larvae}}{\text{m}^2\text{phloem}}\right)\left(\frac{\text{m}^2 \text{ phloem}}{\text{tree}}\right)(\text{proportion of infested trees})\#(\text{S3.10})$$

In this calculation we assume that the density of larvae in the phloem is equal all over the tree. We then use the equation found in Fig (2) of,

$$Y = 0.024 \text{ x}^2 - 0.307 \text{ x} + 2.63$$

where Y is the m^2 phloem of a tree and x is the DBH, diameter at breast height, in cm.

to calculate $\left(\frac{\text{m}^2 \text{ phloem}}{\text{tree}}\right)$. We find that for the data shown (2 sites) the amount of phloem per square meter per tree is

Site	Mean DBH	m^2 per tree
1	17.8	4.7696
2	21.5	7.0935

In (Siegert et al., 2010) the authors fitted

$$P_B = 1 - e^{-c_B L}$$

Where P_B is the probability detect an infested tree using underbark inspections, L is the larvae per m^2 and c_B is the constant. The values of c_B given for these two sites are 0.16, 0.13 for site 1 and 2, respectively. Transforming the L measure to larvae per tree we scale the value of c_B by dividing by (m^2 phloem per tree) (fraction of the trees infested) to obtain

Site 1, $c_B = 0.045$

Site 2, $c_B = 0.031$

So, taking the average for site 1 and 2 we get $c_B = 0.038$.

S4: OPTIMISATION ALGORITHM

The optimisation algorithm randomly selects the required number of sites and calculates the mean probability of detection, $p(\Omega,n,\Delta t)$, for the given sampling arrangement Ω_j (under the given surveillance parameters, $n,\Delta t$), as described in the main text. We then use this detection probability as the 'objective function' in the optimisation algorithm, which needs to be maximised for detecting at least one adult beetle. For a prespecified number of iterations (J), the algorithm proceeds by sequentially replacing a single site with another randomly selected before calculating the objective function again. The arrangement with the new site is then either accepted or rejected before another site is randomly replaced and the process is repeated. Each time, the following Metropolis criterion is used to estimate the probability of accepting the new site:

$$P(\Omega_j \to \Omega_{j+1}) = 1 \text{ if } p(\Omega_{j+1},n,\Delta t) > p(\Omega_j,n,\Delta t)$$

$$P(\Omega_j \to \Omega_{j+1}) = \exp\left(\frac{p(\Omega_{j+1},n,\Delta t) - p(\Omega_j,n,\Delta t)}{temp_j}\right) \text{ if } p(\Omega_{j+1},n,\Delta t) < p(\Omega_j,n,\Delta t)$$

If the objective function was equal between iterations, then the new arrangement was accepted with a probability of 0.5. The 'temperature' of the algorithm (`temp`) is multiplied by the cooling rate (`alpha`) at the end of each iteration (i.e., an exponential cooling schedule). The result of this is that in the early stages of the algorithm, `temp` is high and so is the probability of accepting 'worse' arrangements of sampling sites - thereby encouraging a full exploration of the full parameter space, avoiding any local maxima. As the algorithm progresses, `temp` decreases and it becomes increasingly likely that worse arrangements are rejected (although there initially remains some freedom to explore the parameter space). In the late stages of the algorithm, all arrangements which give a lower probability of detection are rejected, allowing a good approximation of the true optimal arrangement to be found.

S5: Quantification of sample location spread

To quantify the relative spread of surveillance locations we used the metric proposed by Greig-Smith (Greig-Smith, 1952; Martín et al., 2018). Greig-Smith observed that if individual locations of an object of interest (in this instance surveillance locations) were distributed at random, their counts in grid cells (or quadrats) would have a Poisson distribution with the mean equal to the variance. A "patchy" distribution has a variance larger than its mean. We used the method to quantify the relative spread of surveillance locations shown in Figures 3 and 4. We counted the number of surveillance locations in grid cells of size 10 km x 10 km and calculated the variance:mean ratio. The results show that there is much greater patchiness in the REPS locations compared with those that are optimised, and that generally, optimised surveillance for girdled trees is more spread than optimised surveillance for trap locations. We also note that as the time frame for detection increases, the optimised locations of the traps become more spread (i.e. less patchy).

Table S5: Quantification of the relative spread of surveillance locations

Simulation description	Variance of counts / mean of counts	Figure reference
Girdled tree locations optimised for detection within 8 years for the scenario where EAB entry pathway certainty is 70%	1.44	Fig 3A
Trap locations optimised for detection within 8 years for the scenario where EAB entry pathway certainty is 70%	1.67	Fig 3B
REP locations for the scenario where EAB entry pathway certainty is 70%	5.61	Fig 3C
Girdled tree locations optimised for detection within 8 years for the scenario where EAB entry pathway certainty is 50%.	1.63	Fig 4A
Girdled tree locations optimised for detection within 4 years for the scenario where EAB entry pathway certainty is 50%.	2.30	Fig 4A
Girdled tree locations optimised for detection within 2 years for the scenario where EAB entry pathway certainty is 50%.	2.32	Fig 4A
Trap locations optimised for detection within 8 years for the scenario where EAB entry pathway certainty is 50%.	1.73	Fig 4B
Trap locations optimised for detection within 4 years for the scenario where EAB entry pathway certainty is 50%.	2.81	Fig 4B
Trap locations optimised for detection within 2 years for the scenario where EAB entry pathway certainty is 50%.	2.61	Fig 4B
REP locations for the scenario where EAB entry pathway certainty is 50%	5.61	Fig 4B

S6: Model validation of the invasion and spread of the Emerald Ash Borer in Great Britain (EAB; *Agrilus Planipennis*)

We built a spatially explicit model of the invasion and spread of the Emerald Ash Borer (EAB) in Great Britain. Like in many predictive models, only partial validation is possible, as to date there is no evidence of the EAB presence in the UK to compare the dynamics to. Therefore, to validate the population dynamics and spread, we compare our simulation results where we used data from (Duan et al., 2013; Mercader et al., 2009; Orlova-Bienkowskaja & Volkovitsh, 2018; Showalter et al., 2020; Ward et al., 2020; Webb et al., 2021) with data from EAB infestations in the USA (Duan et al., 2015; Knight et al., 2013; McCullough et al., 2019; Siegert et al., 2010b, 2021; Steiner et al., 2019). We looked at four components of the population dynamics: EAB net population growth rates, ash tree mortality, number of larvae per tree, and EAB spatial dispersal.

S6.1 EAB calculation of net population growth rates (R_0)

(Duan et al., 2015) calculated the EAB net population growth rates (R_0) across several sites from 2008-2014. For trees with no parasitism, the average across years was approximately 2.93. We simulated the EAB population dynamics over time using our model for 10,000 realisations of the model. The mean simulated population growth rates decrease and start to plateau as time from incursion increases. The rates are similar to those observed by Duan et al., (2015).
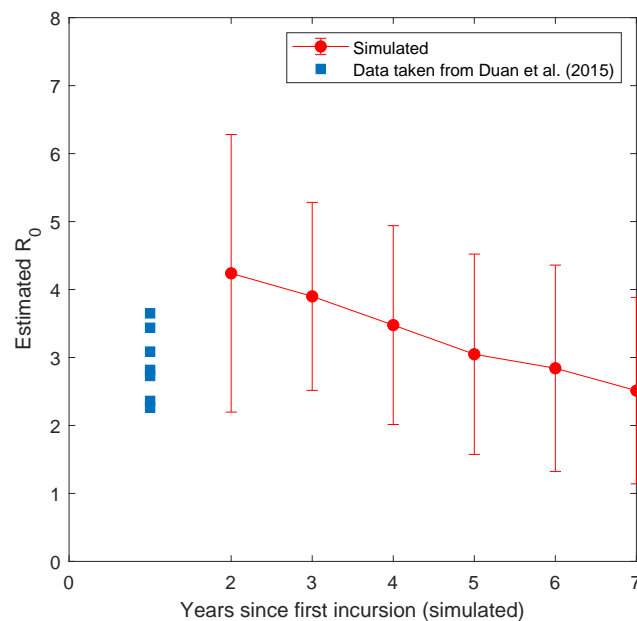

Fig S6.1 Estimated values of net population growth rate. The error bars show the $\pm$ the standard deviation from the mean. The blue squares on the y-axis are the estimates taken from Duan et al., (2015).

S6.2 Ash tree mortality
In (Siegert, Engelken, & McCullough, (2021), a larval density of 49.2% is recorded in infected ash trees. After four years nearly all trees had died. Fig S4.2 shows the average outcome from 10,000 realisations of the simulation $\pm$ standard deviation with the data from (Siegert et al.,

2021) adjusted so first observations of ill health accord. Although we cannot be certain of when the first incursions occurred in the US data, this shows that the modelled rates of tree decline are plausible.
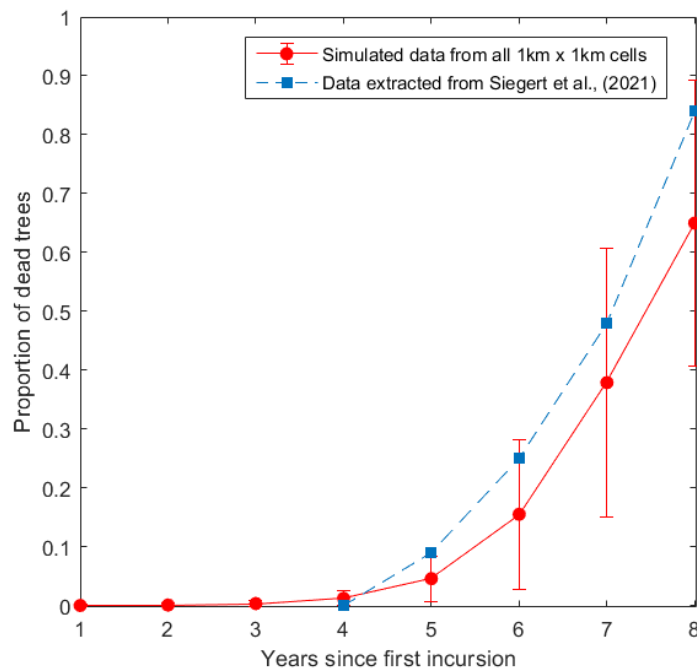

Fig S6.2 Proportion of killed trees by EAB infestation by year. The red symbols are modelled, and the blue squares are based on data reported in Siegert et al. (2021).

S6.3 Number of larvae per tree over time

McCullough et al., (2019) estimated the densities of EAB larvae in ash trees. We compared their results with the results of the population dynamics model for two values of θ (the proportion of univoltine larvae). The results show that our model reproduces reasonable values of the number of larvae per square meter over time.
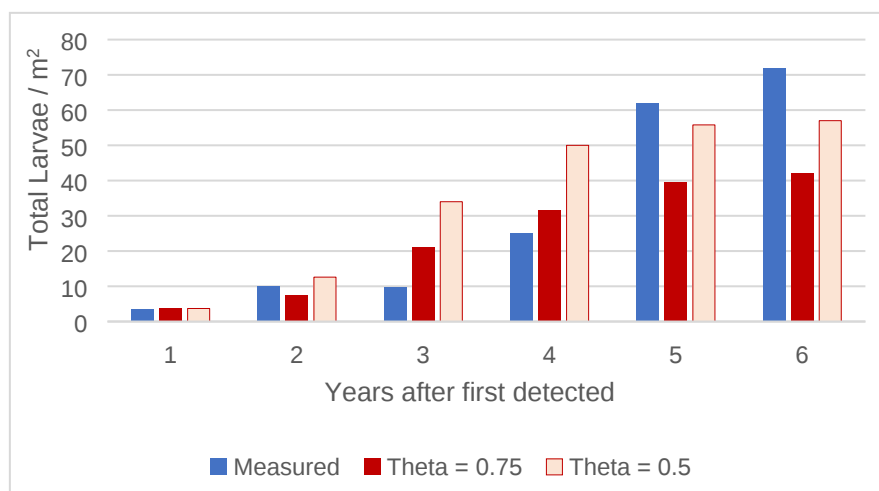

Fig S6.3 The mean total EAB observed (larval galleries) and predicted EAB larvae. The measured data from trees not treated with insecticide was reproduced from McCullough et al., (2019). The simulated relate to two values of theta (the proportion of semivoltine larvae).

S6.4 EAB spatial dispersal

The USDA reports that natural spread is typically between 0.8 km – 10 km per year (https://www.aphis.usda.gov/sites/default/files/eab-manual.pdf). Data from (Siegert et al., 2014) suggests an average rate of spread, allowing for satellite jumps, of approximately 20 km per year during the initial 5-year period. (Webb et al., 2021) combined data from North American studies and estimated an average rate of spread of 47 km per year after EAB establishment. We ran 10,000 random realisations of our simulation and calculated the average increase in distance from the epicentre from the 5th to 8th year of the invasion. The average spread rate at this point in the epidemic was 46.2 km per year (reflecting the parameterisation and the data), however, there were a range of outcomes (Fig S6.4) dependent on the local host and the stochastic nature of the spread.
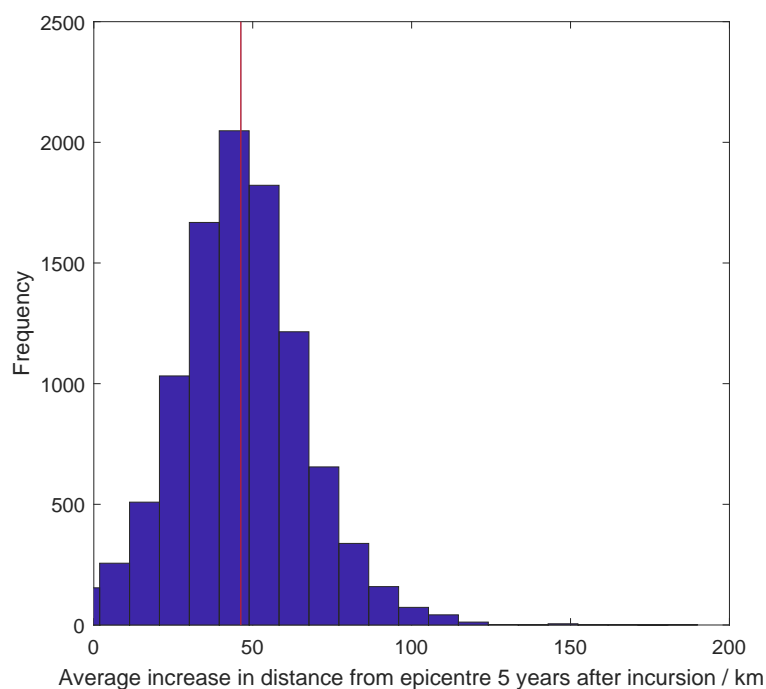

Fig S6.4 A histogram of the simulated average increase in distance from the epicentre after 5 years from the first incursion.

S7: Simulations with higher dispersal rates and bigger proportions of semivoltine larvae

We ran further simulations to determine the sensitivity of our results to increasing the natural dispersal parameter and changes to the proportion of semivoltine larvae in the beetle population.

The scenario simulated is the scenario where knowledge of entry pathways is 50% for detection within 8 years and for 500 devices. We analysed simulations for increased dispersal rates (25%, 50% and 100% increase) and increased proportions of semivoltine larvae (25%, 50% and 95%).

In line with the results from the main text, increasing the natural dispersal (Fig S7.1) or the percentage of univoltine larvae (Fig S7.2) results in the population establishing faster. This increases the probability of detection both through REPS and optimised sampling. The improvement associated with the optimised design increases marginally with dispersal (Table S7).
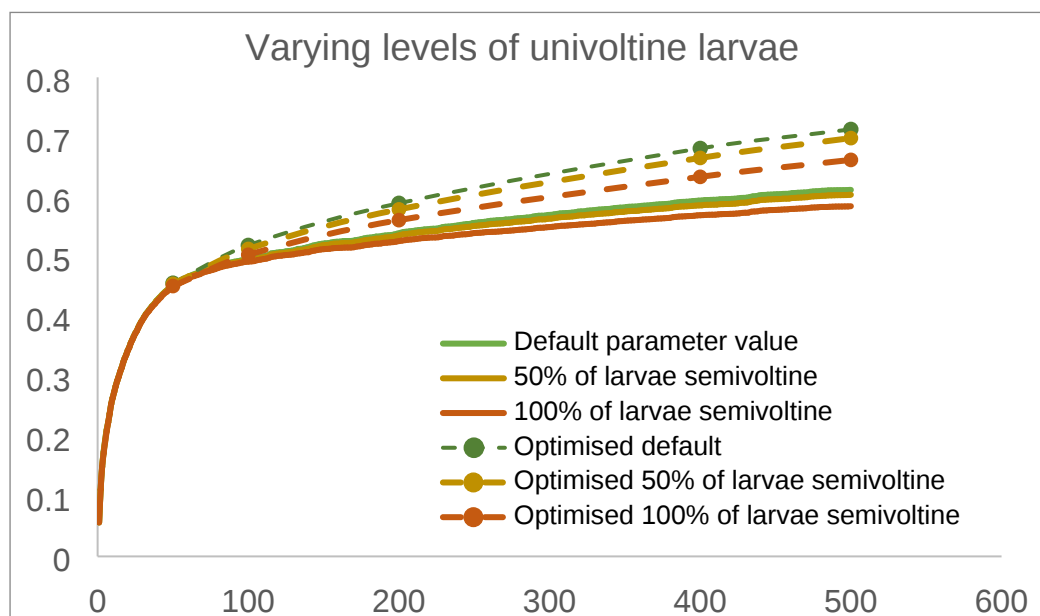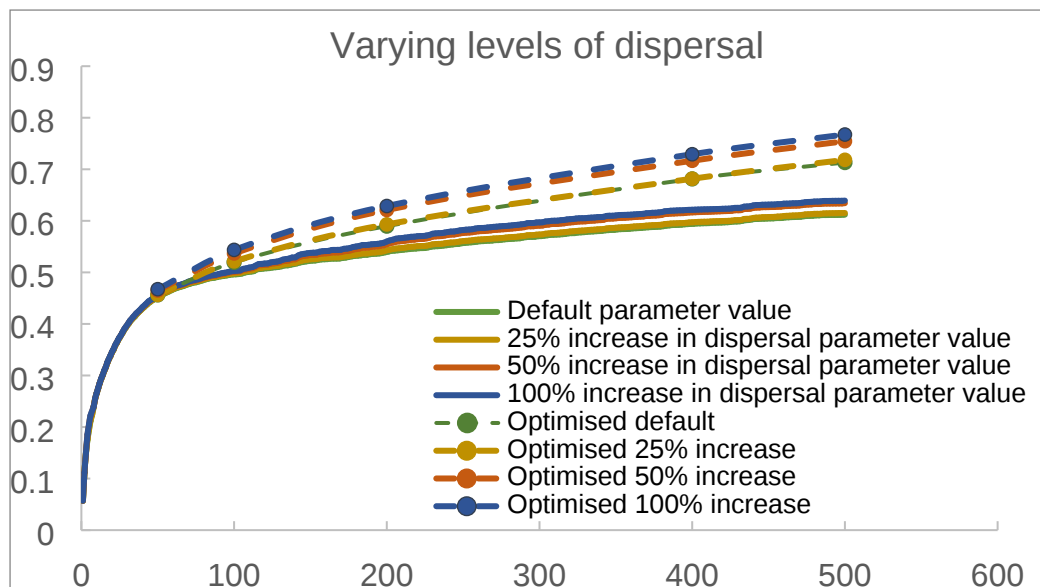
Table S7: The percentage increase in the probability of detecting when using an optimised strategy compared with REPS for the 50:50 scenario.

	Number of sample locations				
	50	100	200	400	500
Default parameters	0.87	4.69	9.29	14.66	16.51
25% increase in dispersal parameter	0.61	4.69	9.60	14.68	16.75
50% increase in dispersal parameter	2.07	7.16	12.30	16.73	18.94
100% increase in dispersal parameter	2.40	8.16	12.71	17.99	20.04
50% larvae are semivoltine	0.78	3.83	8.40	13.91	16.10
95% larvae are semivoltine	0.32	2.33	6.85	11.51	13.56

Bibliography

Duan, J. J., Bauer, L. S., Abell, K. J., Ulyshen, M. D., & Van Driesche, R. G. (2015). Population dynamics of an invasive forest insect and associated natural enemies in the aftermath of invasion: implications for biological control. *Journal of Applied Ecology*, *52*(5), 1246–1254. https://doi.org/10.1111/1365-2664.12485

Duan, J. J., Larson, K., Watt, T., Gould, J., & Lelito, J. P. (2013). Effects of host plant and larval density on intraspecific competition in larvae of the emerald ash borer (Coleoptera: Buprestidae). *Environmental Entomology*, *42*(6), 1193–1200. https://doi.org/10.1603/EN13209

Greig-Smith, P. (1952). The Use of Random and Contiguous Quadrats in the Study of the Structure of Plant Communities. *Annals of Botany*, *16*(62), 293–316. https://www.jstor.org/stable/42907156

Knight, K. S., Brown, J. P., & Long, R. P. (2013). Factors affecting the survival of ash (Fraxinus spp.) trees infested by emerald ash borer (Agrilus planipennis). *Biological Invasions*, *15*(2), 371–383. https://doi.org/10.1007/s10530-012-0292-z

Martín, C. S., Milne, A. E., Webster, R., Storkey, J., Andújar, D., Fernández-Quintanilla, C., & Dorado, J. (2018). Spatial Analysis of Digital Imagery of Weeds in a Maize Crop. *ISPRS International Journal of Geo-Information 2018, Vol. 7, Page 61*, *7*(2), 61. https://doi.org/10.3390/IJGI7020061

McCullough, D. G., Poland, T. M., Tluczek, A. R., Anulewicz, A., Wieferich, J., & Siegert, N. W. (2019). Emerald Ash Borer (Coleoptera: Buprestidae) Densities over a 6-yr Period on Untreated Trees and Trees Treated with Systemic Insecticides at 1-, 2-, and 3-yr Intervals in a Central Michigan Forest. *Journal of Economic Entomology*, *112*(1), 201–212. https://doi.org/10.1093/jee/toy282

McCullough, D. G., & Siegert, N. W. (2007). Estimating Potential Emerald Ash Borer (Coleoptera: Buprestidae) Populations Using Ash Inventory Data. *Journal of Economic Entomology*, *100*(5), 1577–1586. https://doi.org/10.1093/jee/100.5.1577

Mercader, R. J., McCullough, D. G., & Bedford, J. M. (2013). A Comparison of Girdled Ash Detection Trees and Baited Artificial Traps for Agrilus planipennis (Coleoptera: Buprestidae) Detection . *Environmental Entomology*, *42*(5), 1027–1039. https://doi.org/10.1603/en12334

Mercader, R. J., Siegert, N. W., Liebhold, A. M., & McCullough, D. G. (2009). Dispersal of the emerald ash borer, Agrilus planipennis, in newly-colonized sites. *Agricultural and Forest Entomology*, *11*(4), 421–424. https://doi.org/10.1111/j.1461-9563.2009.00451.x

Mercader, R. J., Siegert, N. W., & Mccullough, A. D. G. (2012). Estimating the Influence of Population Density and Dispersal Behavior on the Ability to Detect and Monitor Agrilus planipennis (Coleoptera: Buprestidae) Populations. *J. Econ. Entomol*, *105*(1), 272–281. https://doi.org/10.1603/EC11172

Orlova-Bienkowskaja, M. J., & Volkovitsh, M. G. (2018). Are native ranges of the most destructive invasive pests well known? A case study of the native range of the emerald ash

borer, Agrilus planipennis (Coleoptera: Buprestidae). *Biological Invasions*, *20*(5), 1275–1286. https://doi.org/10.1007/S10530-017-1626-7

Showalter, D. N., Saville, R. J., Orton, E. S., Buggs, R. J. A., Bonello, P., & Brown, J. K. M. (2020). Resistance of European ash (Fraxinus excelsior) saplings to larval feeding by the emerald ash borer (Agrilus planipennis) . *Plants, People, Planet*, *2*(1), 41–46. https://doi.org/10.1002/ppp3.10077

Siegert, N. W., Engelken, P. J., & McCullough, D. G. (2021). Changes in demography and carrying capacity of green ash and black ash ten years after emerald ash borer invasion of two ash-dominant forests. *Forest Ecology and Management*, *494*, 119335. https://doi.org/10.1016/J.FORECO.2021.119335

Siegert, N. W., Mccullough, D. G., Liebhold, A. M., & Telewski, F. W. (2014). Dendrochronological reconstruction of the epicentre and early spread of emerald ash borer in North America. *Diversity and Distributions*, *20*(7), 847–858. https://doi.org/10.1111/DDI.12212

Siegert, N. W., McCullough, D. G., Williams, D. W., Fraser, I., Poland, T. M., & Pierce, S. J. (2010a). Dispersal of Agrilus planipennis (Coleoptera: Buprestidae) From Discrete Epicenters in Two Outlier Sites. *Environmental Entomology*, *39*(2), 253–265. https://doi.org/10.1603/EN09029

Siegert, N. W., McCullough, D. G., Williams, D. W., Fraser, I., Poland, T. M., & Pierce, S. J. (2010b). Dispersal of Agrilus planipennis (Coleoptera: Buprestidae) From Discrete Epicenters in Two Outlier Sites. *Environmental Entomology*, *39*(2), 253–265. https://doi.org/10.1603/EN09029

Steiner, K. C., Graboski, L. E., Knight, K. S., Koch, J. L., & Mason, M. E. (2019). Genetic, spatial, and temporal aspects of decline and mortality in a Fraxinus provenance test following invasion by the emerald ash borer. *Biological Invasions*, *21*(11), 3439–3450. https://doi.org/10.1007/s10530-019-02059-w

Ward, S. F., Fei, S., & Liebhold, A. M. (2020). Temporal dynamics and drivers of landscape-level spread by emerald ash borer. *Journal of Applied Ecology*, *57*(6), 1020–1030. https://doi.org/10.1111/1365-2664.13613

Webb, C. R., Mona, T., & Gilligan, C. A. (2021). Predicting the potential for spread of emerald ash borer (Agrilus planipennis) in Great Britain: What can we learn from other affected areas? *Plants, People, Planet*, *March*, 1–12. https://doi.org/10.1002/ppp3.10195